International Journal of Automotive Technology, Vol. 21, No. 3, pp. 685–690 (2020)
DOI 10.1007/s12239–020–0066–z

pISSN 1229–9138/ eISSN 1976–3832

OPTIMUM PLACEMENT OF THE 3-AXIS LF ANTENNA IN A SMALL MOBILE DEVICE FOR VEHICULAR APPLICATIONS

Jun Hur[1)], Tae Heung Lim[2)] and Hosung Choo[2)*]

[1)]Metamaterial Electronic Device Research Center, Hongik University, Seoul 08826, Korea
[2)]School of Electronic and Electrical Engineering, Hongik University, Seoul 08826, Korea

(Received 23 October 2018; Revised 21 March 2019; Accepted 1 August 2019)

ABSTRACT–This paper proposes the optimum placement of an LF antenna in a small mobile device to minimize coverage range degradation of a PASE system. The small mobile device, vehicle, and 3-axis LF antenna are modeled as piecewise triangular meshes and simulated using a full-wave electromagnetic simulator to verify the feasibility of mounting the LF antenna in a small device. We then find the optimum placement of the 3-axis LF antenna inside the mobile device to maximize the coverage range of the system. Finally, the received power of the 3-axis LF antenna is analyzed in conjunction with the PASE system for vehicle application to accurately estimate the system performance. The results demonstrate that the position optimization of the LF antenna in the small mobile device is capable of maximizing the coverage range of the PASE system.

KEY WORDS : Passive access system entry, LF antenna, Mobile device, Optimum placement, Readable volume

1. INTRODUCTION

The passive access system entry (PASE) has been widely used for access control of vehicles, for example, opening the doors and trunk, engine control, and seat positioning without manipulating the vehicle keys by hand (Waraksa *et al*., 1990; Diem, 2001; Alrabady and Mahmud, 2005). The frequency commonly used in PASE systems for signal transmission from the vehicle to the smart key is the low frequency (LF) at 125 kHz because the LF frequency has the advantages of low transmission loss and high penetration due to the large wavelength. The typical LF band antenna used in the PASE system is a coil antenna employing a ferrite core, and the maximum coverage range of the system is predominantly determined by the magnetic field distributions of the LF antenna. In order to increase the maximum coverage range of the PASE system, some previous studies have been focused on generating an omni-directional field pattern using multiple bar type LF antennas (John *et al*., 2003; Sato and Sano, 2014). In addition, to enhance the field strength of the LF antenna, researches on the optimum shape of the ferrite core, the material, and the number of the coil turns have been extensively carried out (Poole, 2004; Maguire and Robertson, 2015). Recently, the study on the estimation of the coverage range has been conducted for the performance verification of the PASE system according to the LF antenna location inside the vehicle (Brzeska and Chakam, 2007; Takas *et al*., 2009). Although these LF antennas exhibit good performance in free space, the pattern distortion occurs due to the finite platform effect, resulting in a reduced coverage range, particularly when the LF antennas are mounted in a small platform such as a smart key and a mobile device (Kim *et al*., 2018; Lee and Lee, 2018). Therefore, in order to mount the PASE system in a small mobile device and to improve the maximum coverage range, an in-depth study on the platform effect according to the mounting position of the LF antenna is needed. More sophisticated studies should also be performed in advance to effectively minimize the conventional bar type LF antennas.

In this paper, we demonstrate the feasibility of mounting the miniaturized 3-axis LF antenna in a small mobile device and optimize the mounting position of the LF antenna in a small mobile device to minimize the field pattern distortion that degrades the coverage range of the system. Since the mounting space in the mobile device is narrow, the 3-axis LF antenna which consists of one polyhedron ferrite core and coils wound in three directions is used to minimize the antenna size. To estimate the coverage of the 3-axis LF antenna in the PASE system mounted on a small mobile device, we simulate the LF antenna, mobile device, and commercial vehicle using the FEKO EM simulator (EM Software and Systems, 2018). The main antenna characteristics such as field distributions and received power are investigated to observe the performance variation according to the position in a small mobile device. Then, we find the optimum placement of the 3-axis LF antenna inside the mobile device to maximize the coverage range of the system. In addition, the

**Corresponding author*. e-mail: hschoo@hongik.ac.kr

received power of the 3-axis LF antenna mounted at the optimum position inside the mobile device is analyzed while varying the distance from the vehicle. The results confirm that the position optimization of the LF antenna in the small mobile platform is essential to maximize the coverage range of the PASE system.

2. 3-AXIS LF ANETNNA

In general, an LF antenna using the mutual inductance between the coils typically has a bar type core, and coils are wound only in one axial direction along the core. When such an LF antenna is applied to hand held devices such as vehicle smart keys, multiple numbers of the bar type LF antennas are used to cover all three directions. In this work, we apply this LF antenna system in a small device such as a mobile device, in which the space for the LF antenna is not sufficient to mount the conventional multiple bar type LF antennas. Therefore, we proposed a single 3-axis LF antenna which uses a single ferrite core with coils wound in three directions to minimize the antenna size. This proposed 3-axis LF antenna can allow installation in small mobile devices which is difficult with commercial bar type LF antennas. Figure 1 shows the proposed geometry of a 3-axis LF antenna consisting of multi-turn coils wound along each of the three axes (*x*-, *y*-, *z*-axis) and a polyhedron ferrite core ($\mu_r = 400$, $\tan\delta = 0.003$) with dimensions of d_1, d_2 and d_3, and h_f. The loss tangent ($\tan\delta = 0.003$) of the ferrite core is considered as the magnetic loss tangent at 125 kHz. However, this loss tangent does not seriously affect the field distributions of the LF antenna. We tried to design the proposed 3-axis LF antenna to have an inductance of 7.2 mH which can be fully matched to the system circuit having a 225 pF capacitor and a 150 kΩ resistor in parallel. The coils are wound 200 times on each *x*-, *y*-, and *z*-axis to have an inductance of 7.5 mH between the beginning and the end of the *x*- and *y*- coils and the value of the *z*-coil is 6.7 mH. The outsides of the coils are coated with 25 μm thick polyethylene ($\varepsilon_r = 2.25$, $\tan\delta = 0.04$) to insulate the coils and core. The miniaturization of the antenna can be achieved by the shape of the polyhedron ferrite core because this shape allows the coils of three axes to be wound around a single core. The *x*- and *y*-axis coils are wound perpendicularly along the ferrite core having a dent of a depth d_3 and a width of d_2. The *z*-axis coil is then wound on the lateral side of the core with a width of $d_1 + d_2$. The detailed design parameters are listed in Table 1.

Figure 2 presents the Poynting vectors at the plane $z = 0$ mm (-2 m $\le x, y \le 2$ m) of the 3-axis LF antenna. We

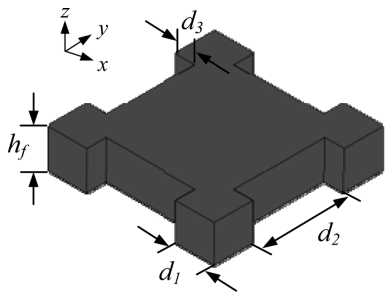

(a) Perspective view of the ferrite core

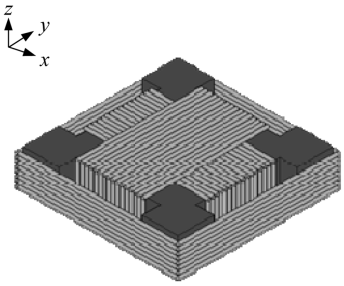

(b) Perspective view of the 3-axis LF antenna with multi-turn coils

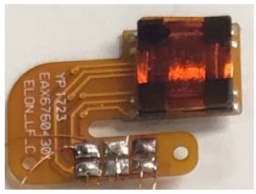

(c) Photograph of the fabricated 3-axis LF antenna

Figure 1. Geometry of the 3-axis LF antenna.

analyze the *x*-, *y*-, *z*-, and total component to ensure that the field distribution of each component is well formed symmetrically. Each *x*-, *y*-, and *z*-coil including the matching circuit is excited by the VS-220Q signal generator of the TESTLINK with 12 V at 125 kHz. Then, the Transponder Evaluation and Development (TED) Kit 2 (NXP, 2016) is used to test the reading distance of the LF antenna, and we measure the threshold Poynting vector strength of the LF antenna at the maximum reading distance. Experimentally, the resulting maximum reading distance of approximately 83 cm along the *x*-axis is measured at the same height ($z = 0$ m) with the LF antenna, where the threshold Poynting vector strength is -160 dBW/m^2. The threshold value can be changed arbitrarily

Table 1. Specifications of the 3-axis LF antenna.

Specifications	d_1	d_2	d_3	h_f	Ferrite permeability	Coil turns (*x*-, *y*-, *z*-axis)	Wire coating	Coating thickness
Value	1.25 mm	4.5 mm	0.63 mm	2 mm	400	200	Polyethylene ($\varepsilon_r = 2.25$, $\tan\delta = 0.04$)	25 μm

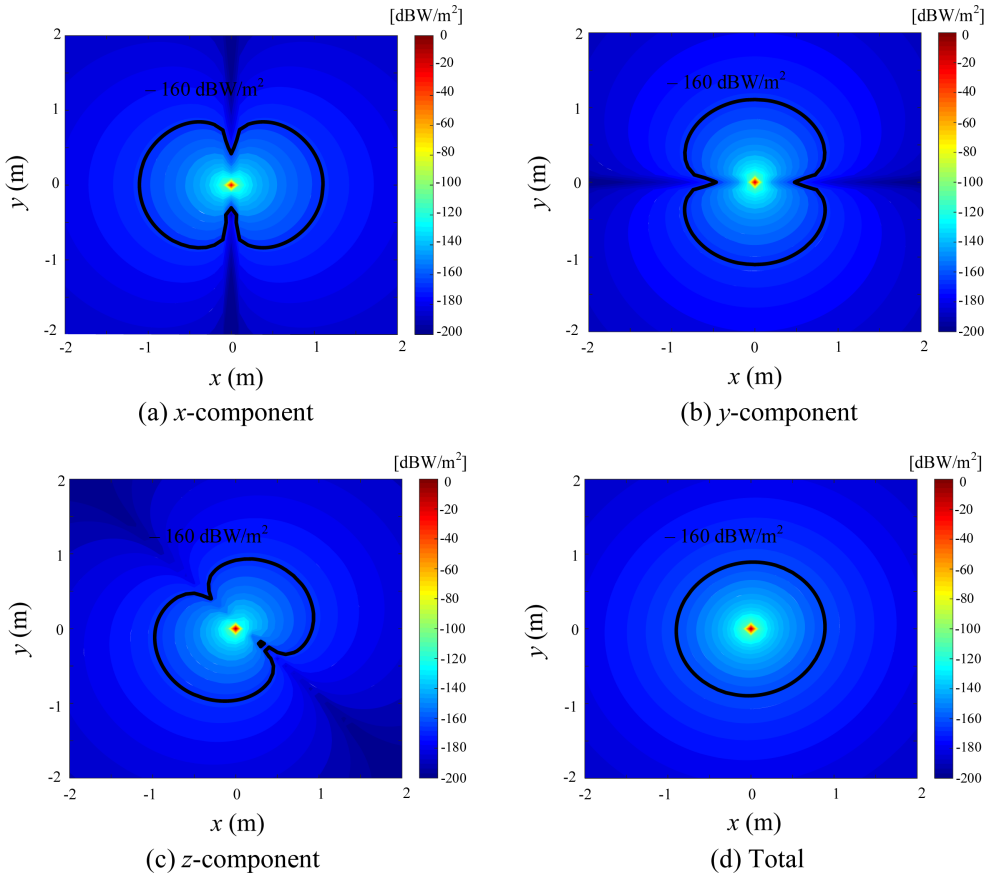

Figure 2. Poynting vectors of the 3-axis LF antenna.

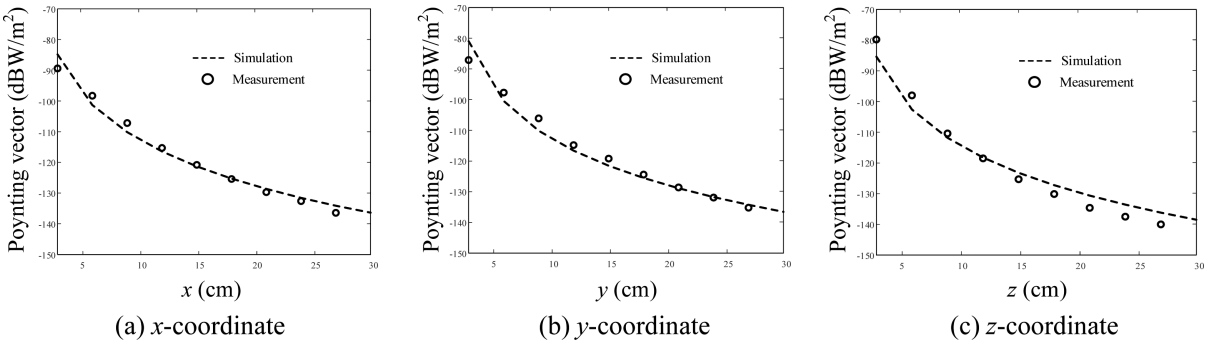

Figure 3. Poynting vectors of the 3-axis LF antenna according to the distance.

depending on the performance of the test bed system. In the figure, the boundaries of the threshold Poynting vector strength of – 160 dBW/m^2 are represented by bold lines. As can be seen, in the plane with z = 0 mm, there is the readable area where the Poynting vector value is larger than the threshold Poynting vector of – 160 dBW/m^2, and the surface area of the reading zone is around 0.7 m^2.

Figure 3 shows the simulated Poynting vector as a dashed line in comparison with the measured results of the 3-axis LF antenna indicated by circles. We measured the Poynting vectors by using the MS2720T spectrum analyzer (Anritsu, 2016) with an EM-6992 magnetic probe (ETS-Lindgren, 2016). The measured Poynting vector strengths along the x-, y-, and z-axis from the 3-axis LF antenna show a good agreement with the simulated results.

3. OPTIMUM PLACEMENT OF THE 3-AXIS LF ANTENNA AND VERIFICATION IN VEHICULAR APPLICATIONS

Figure 4 shows the geometry of the mobile device with dimensions of $l_1 \times l_2 \times h_p$ mm^3 (161.4 × 68.8 × 7.9 mm^3).

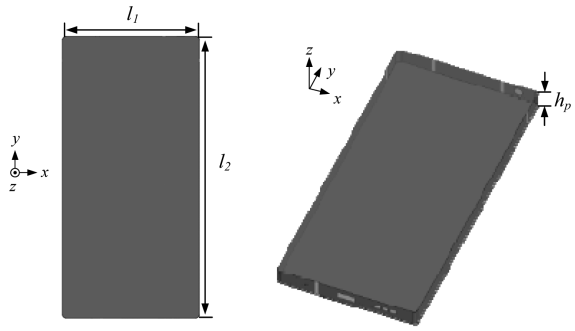

Figure 4. Geometry of the small mobie device.

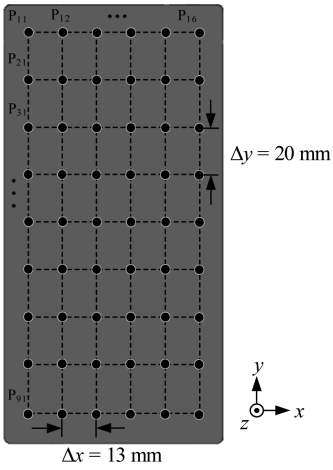

Figure 5. Mountable positions of the mounted 3-axis LF antenna in a mobile device.

The mobile device consists of the hexahedron perfect electric conductor (PEC) with several slots on the sides for ear jacks, speakers, and buttons. As shown in Figure 5, we find the optimum mounting position among the available positions inside the mobile device, indicated by the grid points with spacings of 13 mm and 20 mm in *x*- and *y*-directions, respectively.

Figure 6 presents the simulated readable volumes of the 3-axis LF antenna according the mounting positions. The

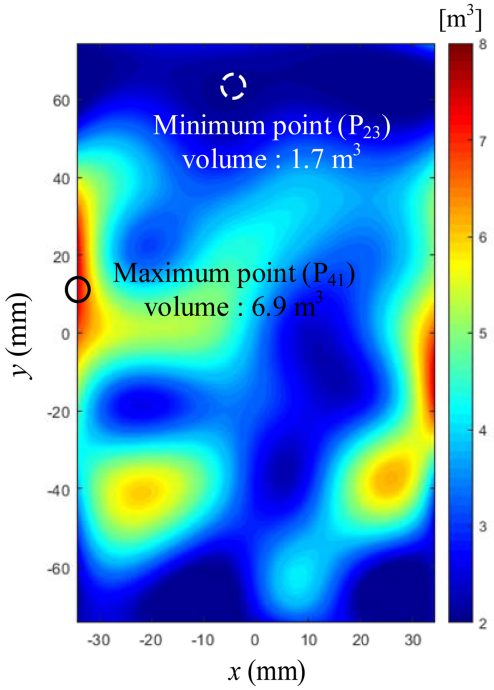

Figure 6. Readable volume of the mounted 3-axis LF antenna in a mobile device.

maximum and minimum readable volumes of 6.9 m^3 and 1.7 m^3 are obtained at the grid points P_{41} and P_{23} respectively. These results confirm that the optimization of the mounting position can minimize the field pattern distortion that degrades the coverage range of the PASE system.

Figure 7 shows a contour plot of the threshold Poynting vectors on the z = 0 mm plane when the 3-axis LF antenna is located at the optimum (solid line) and worst locations (dashed line). As can be seen, the z-component of the 3-axis LF antenna in the small mobile device is most affected by the placement positions compared with the x- and y-components.

To verify the coverage range of the PASE system in a vehicle application, the received power of the 3-axis LF antenna is analyzed when a bar type LF antenna is installed

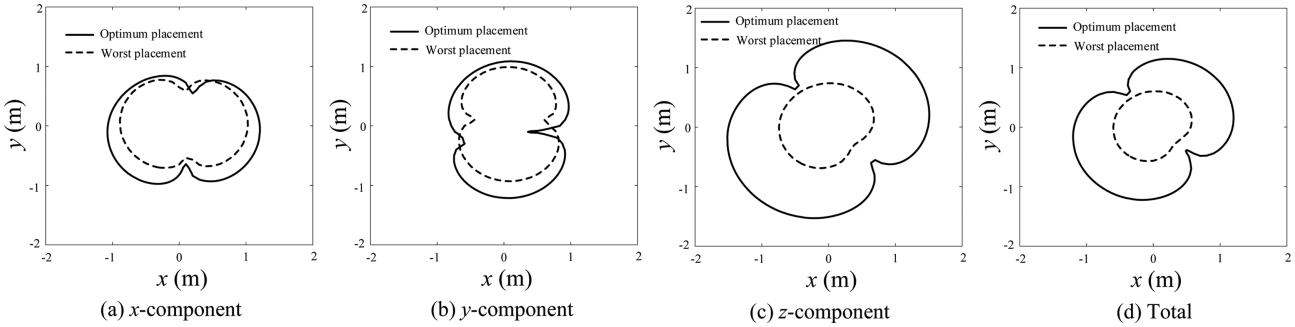

Figure 7. Contour plot of the threshold Poynting vectors according to mounting positions.

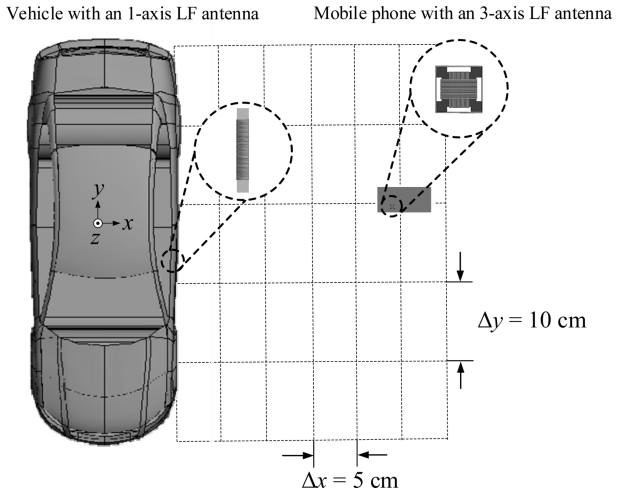

Figure 8. Locations of the mobile device with a 3-axis LF antenna in a vehicle application.

in a vehicle as shown in Figure 8. The commercial vehicle has overall dimensions of 1.68 × 4.69 × 1.88 m^3 (width × length × height), and the bar type LF antenna is mounted on the door handle of the vehicle. To estimate the received power of the 3-axis LF antenna, the location of the small mobile device is moved to the grid points with spacings of 50 cm and 100 cm in the *x*- and *y*- directions. Figure 9 shows the simulated and measured Poynting vectors of the 1-axis LF antenna mounted on the vehicle. For the *x*-, *y*-, and *z*- coordinates, the distance from the 1-axis LF antenna are verified with the measurement.

Figure 10 presents the simulated received power of the 3-axis LF antenna according to the locations of the small mobile device outside the vehicle, where the antenna is at an optimum position inside the small mobile device. The strength of the received power is – 120 dBm at a distance of 1 m boundary, and the power reduced to – 160 dBm at a range of 4 m as indicated by the dotted line. The coverage range of the PASE system can be effectively verified through this EM analysis which is a variation of the received power strength of the 3-axis LF antenna.

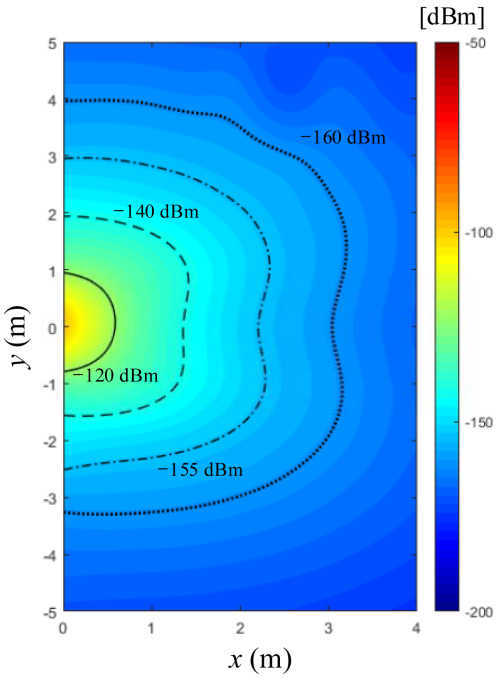

Figure 10. Received power of the 3-axis LF antenna according to the locations based on the vehicle.

4. CONCLUSION

We have investigated the feasibility of mounting the 3-axis LF antenna in a small mobile device and optimized the antenna position to maximize the coverage range of the PASE system. The commercial vehicle, mobile device and LF antennas were modeled in the FEKO EM simulator to estimate the antenna characteristics, such as the field distributions and received power. The optimum placement was found by evaluating the readable volume at mountable positions inside the mobile device, and the results showed that the maximum readable volume value was 6.9 m^3 at the optimum placement while the value at worst placement was 1.7 m^3. In addition, the received power of the 3-axis LF antenna mounted at the optimum placement inside the

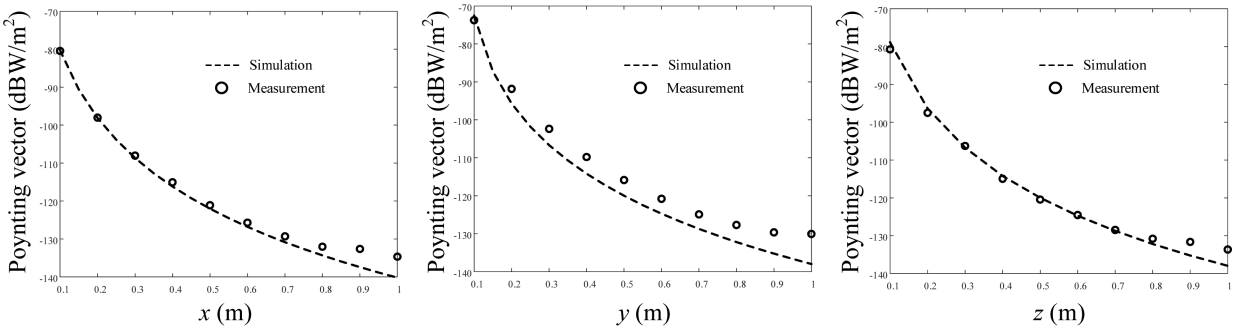

(a) *x*-component (b) *y*-component (c) *z*-component

Figure 9. Contour plot of the threshold Poynting vectors according to mounting positions.

mobile device were analyzed to accurately certify the coverage range of the system. The results demonstrate that the optimization of the LF antenna position in a small mobile device could maximize the coverage range of the PASE system, and the full-wave EM simulation for estimating the antenna characteristic with platforms such as mobile device and vehicle is essential to verify the performance of the system effectively.

ACKNOWLEDGEMENT–This work was supported by the National Research Foundation of Korea (NRF) grant funded by the Korea government (Basic Research) (No. NRF-2017R1D1A1B04031890) and in part by the Basic Science Research Program through the NRF funded by the Ministry of Education (No. 2015R1A6A1A03031833).

REFERENCES

Alrabady, A. I. and Mahmud, S. M. (2005). Analysis of attacks against the security of keyless-entry systems for vehicles and suggestions for improved designs. *IEEE Trans. Vehicular Technology* **54**, **1**, 41−50.

Anritsu (2016). MS2720T. https://www.anritsu.com

Brzeska, M. and Chakam, G. A. (2007). Modelling of the coverage range for modern vehicle access systems at low frequencies. *Proc. 37th European Microwave Conf.*, Munich, Germany.

Diem, W. (2001). Smart card opens the door. *AutoTechnology*, **1**, **1**, 32−33.

EM Software and Systems (2018). FEKO Suite 2018. http://www.altair.com

ETS-Lindgren (2016). EM-6992. https://electrometrics.com

John, S. N., Qignfeng T., Qing, L., Bruce, D. C., Keith, A. W., Artem, M., Ronald, O. K., Riad, G., Matthew, H. and Salman, K. (2003). Remote Access Device Having Multiple Inductive Coil Antenna. U.S. Patent No. 6940461.

Kim, J., Song, S., Shin, H. and Park, Y. (2018). Radiation from a millimeter-wave rectangular waveguide slot array antenna enclosed by a von karman radome. *J. Electromagnetic Engineering and Science* **18**, **3**, 154–159.

Lee, S. and Lee, J. (2018). Calculating array patterns using an active element pattern method with ground edge effects. *J. Electromagnetic Engineering and Science* **18**, **3**, 175–181.

Maguire, S. T. G. and Robertson, P. A. (2015). Low frequency radio polarization sensor with applications in attitude estimation. *IEEE Sensors J.* **15**, **12**, 7304−7311.

NXP (2016). Transponder Evaluation and Development (TED) Kit 2. http://www.nxp.com

Poole, R. (2004). Ferrite Rod Antennas for HF?. BBC R&D White Paper WHP, 91.

Sato, K. and Sano, K. (2014). 3D receptive ultrathin LF band antenna. *Proc. IEEE 3rd Global Conf. Consumer Electronics*, Tokyo, Japan.

Takas, A., Huard, M., Kessler, S., Chakam, G. A. and Lardjane, E. (2009). Estimation of low frequency coverage insidecar for passive access system entry. *Electroincs Letters* **45**, **12**, 596−597.

Waraksa, T., Farley, K., Kiefer, R., Douglas, D. and Gilbert, L. (1990). Passive Keyless Entry System. U.S. Patent No. 5319364.